Article

Not peer-reviewed version

Modulation of Cell Response Through the Covalent Binding of Fibronectin to Titanium Substrates

Parsa Rezvanian , Aroa Alvarez-Lopez , Raquel Tabraue , Rafael Daza , Luis Colchero , Manuel Elices , Gustavo V. Guinea , Daniel González-Nieto , José Pérez-Rigueiro *

Posted Date: 26 May 2023

doi: 10.20944/preprints202305.1870.v1

Keywords: fibronectin; functionalization; activated vapor silanization (AVS); mesenchymal stem cells (MSC); biomaterial.

Article

Modulation of Cell Response through the Covalent Binding of Fibronectin to Titanium Substrates

Parsa Rezvanian [1,2,3], Aroa Álvarez-López [1,2], Raquel Tabraue [1,2], Rafael Daza [1,2], Luis Colchero [1,2], Manuel Elices [2], Gustavo V. Guinea [1,2,4,5], Daniel González-Nieto [1,4,6] and José Pérez-Rigueiro [1,2,4,5,*]

1 Center for Biomedical Technology, Universidad Politécnica de Madrid. 28223 Pozuelo de Alarcón (Madrid) Spain
2 Departamento de Ciencia de Materiales. ETSI Caminos, Canales y Puertos. Universidad Politécnica de Madrid. 28040 Madrid. Spain
3 Department of Animal Biotechnology, Cell Science Research Center, Royan Institute for Biotechnology, ACECR. 8159358686 Isfahan. Iran.
4 Biomedical Research Networking Center in Bioengineering, Biomaterials and Nanomedicine (CIBER-BBN). 28029 Madrid. Spain
5 Instituto de Investigación Sanitaria del Hospital Clínico San Carlos (IdISSC). Calle Prof. Martín Lagos s/n. 28040 Madrid. Spain.
6 Departamento de Tecnología Fotónica y Bioingeniería. ETSI Telecomunicaciones. Universidad Politécnica de Madrid. 28040 Madrid. Spain
* Correspondence: jose.perez@ctb.upm.es; Tel.: +34910674304

Abstract: Titanium (Ti-6Al-4V) substrates were functionalized through the covalent binding of fibronectin, and the effect of the presence of this extracellular matrix protein on the surface of the material was assessed employing mesenchymal stem cell (MSC) cultures. The functionalization process comprised the usage of the activation vapor silanization (AVS) technique to deposit a thin film with a high surface density of amine groups on the material, followed by the covalent binding of fibronectin to the amine groups using the N-(3-dimethylaminopropyl)-N'-ethylcarbodiimide hydrochloride / N-hydroxysuccinimide (EDC/NHS) crosslinking chemistry. The biological effect of the fibronectin on murine MSCs was assessed *in vitro*. It was found that functionalized samples not only showed enhanced initial cell adhesion compared with bare titanium, but also a three-fold increase in the cell area, reaching values comparable to those found on the polystyrene controls. These results represent a clear indication of the potential of modulating the response of the organism to an implant through the covalent binding of extracellular matrix proteins on the prosthesis.

Keywords: fibronectin; functionalization; activated vapor silanization (AVS); mesenchymal stem cells (MSC); biomaterial

1. Introduction

Over the past few decades, there has been an increasing demand for biomaterials that are able to replace various tissues and mimic their functions [1,2]. Titanium (Ti) has been the material of choice for many of these applications owing to its convenient combination of properties: excellent corrosion resistance, relatively low elastic modulus and high tensile strength [3,4]. Due to these excellent properties, titanium biomaterials are suitable candidates for applications as implants and replacement of hard tissue. However, Ti, as it is the case for most if not all of the biomaterials used in the clinical practice, exhibits a major drawback related with the interaction established with the surrounding living tissue: upon implantation the material is not able to form an intimate contact with the adjacent tissues and is covered by a connective tissue capsule. The formation of this connective tissue capsule is a consequence of the foreign body reaction of the recipient organism to the implant. The foreign body reaction implies the activation of the macrophages and, together with active fibroblasts, the generation of a collagen matrix around the implant.[5,6].

The lack of integration with the surrounding tissue of any implant can be problematic, since a weak connection between healthy tissue and implant may lead to infections [7]. Additionally, the

 doi:10.20944/preprints202305.1870.v1

fibrous tissue interface is mechanically weak and causes micro-movements of the implant with respect to the adjacent tissue. These micro-movements can affect the healing process adversely, and lead to the loosening of the implant over time [8,9]. Implant loosening, in turn, may cause pain and often requires revision surgery. For instance, it is reported that the loosening of the implant is the most frequent cause for revision hip arthroplasty [10].

To counteract this problem and facilitate the integration of the material, it is necessary to attract stem cells to the surface of the implant and to promote their activity. Such an approach would result in the formation of the functional tissue directly on the surface of the prosthesis.

Incidentally, a strategy involving surface modification of implants with biomolecules seems adequate and leads to the so-called biofunctionalization of the material. Biofunctionalization consists of modifying the surface of the material, usually through the binding of targeted biomolecules, in an attempt to promote an enhanced biological response of the organism to the implant. It is assumed that this enhanced response is greatly dependent on the existence of specific adhesion sites for different cells at the surface of the material [11]. Although it is possible to immobilize the biomolecules through such simple processes as adsorption or entrapment, the creation of a robust connection between the material and the biomolecule usually requires the formation of a covalent bond which implies the generation of functional groups on the surface of the implant. For instance, in the case of titanium, functionalization is conventionally performed by immersing the substrates inside a solution of an organosilane in an organic solvent, such as pentane or toluene [12–15]. Although this method is simple and facile, it lacks reproducibility and results in the formation of a low surface concentration of functional groups. This is due to the high susceptibility of the silanization reactions to hydrolyzation and oligomerization of the precursor molecules [16,17]. Thus, a functionalization method overcoming these advantages, may greatly improve the biomolecule binding efficacy.

As for the target biomolecule, fibronectin could be of special interest, since it is one of the main insoluble components of the extracellular matrix (ECM). Fibronectin possesses binding sites for heparin, fibrin and collagen [18], as well as several integrin binding sites which may be recognized by different cell lines [19–22]. Fibronectin is found to favor cell adhesion [23,24] and spreading [25,26]. Hence, coating the surface of biomaterials with fibronectin has been a viable strategy for enhancing cellular response to the biomaterials. The positive effect of fibronectin adsorbed on the surface of Ti biomaterials on the cellular response has been addressed previously in various studies. It was reported that adsorption of fibronectin on Ti-6Al-4V alloy from a solution of the protein with a concentration as low as 0.5nM can lead to a significant improvement in the cell attachment to the material [27]. Previously, improved MC3T3-E1 cell adhesion and proliferation on fibronectin-coated Ti was reported by Ku et al. [28]. Adsorption of fibronectin on Ti materials has been demonstrated to improve adhesion and proliferation of human gingival fibroblasts [29], hamster kidney 21C/13 fibroblasts [30], MG63 osteoblasts, C3H10T1/2 mesenchymal stem cells [27], rat bone marrow-derived osteoblast [31] and normal human dermal fibroblasts [32].

In addition to these non-covalent strategies, several procedures for the covalent binding of fibronectin to solid substrates have been developed. Thus, fibronectin was immobilized on Ti alloys using the tresyl chloride chemistry, demonstrating a positive effect on the adhesion of MC3T3-E1 cells [33,34]. In a similar study, Pham et al. functionalized Ti samples using immersion silanization and EDC as crosslinker and concluded that osteoblast-like SaOS2 cells showed better cell adhesion and spreading on fibronectin-decorated samples at 4 h after seeding [35]. These functionalization procedures, however, tend to be extremely dependent on the detailed chemistry of the surface and, consequently, lead to a high variability in the observed outcomes.

In this study, we show how it is possible to covalently bind fibronectin to the surface of biomaterials using a functionalization procedure that is largely independent of the chemistry of the substrate. Ti-6Al-4V is used as a model system and functionalized through the activated vapor silanization (AVS) process, resulting in a high density of reactive amines on the surface of the substrate. Subsequently, fibronectin is bound the functionalized Ti surface through the EDC/NHS

 doi:10.20944/preprints202305.1870.v1

crosslinking chemistry. Lastly, the enhanced response of murine bone marrow mesenchymal stem cells (BM-MSCs) on the fibronectin-decorated titanium samples is verified.

2. Materials and Methods

2.1. Preparation of Ti substrates

Substrates used in this study were cut from an ingot of commercial Ti-6Al-4V alloy with nominal dimensions 10 × 10 × 1 mm. The substrates were polished sequentially with sandpapers grit No. 80, 400, 1200 and 4000. Subsequently, the samples were cleaned by sonication in acetone, isopropanol, distilled water and dried with a flow of argon.

2.1. Covalent immobilization of fibronectin

2.2.1. Functionalization

The surface of the Ti substrates were initially amino-functionalized using the activated vapor silanization (AVS) method, as described elsewhere [36,37]. Briefly, 3-aminopropyltriethoxysilane (APTS, Fluka) is poured inside a closed compartment and evaporated at low vacuum. The vapor is transported by an argon flux (BIP, Purity≥ 99, 9997 %) to an activation chamber where the temperature is risen to 750 ºC. Afterwards, the activated APTS vapor is directed towards the surface of the substrates in the deposition chamber. Finally, the vapor phase is evacuated from the system with a rotary pump. The process is controlled by four parameters: evaporation temperature of APTS (T_{Evap}), activation temperature of APTS (T_{Act}), pressure of argon (P_{Ar}) and deposition time (t). For the functionalization of Ti substrates in this study, the deposition parameters were as follows: T_{Evap} = 150 ºC, T_{Act} = 750 ºC, P_{Ar} = 2 mbar and t =20 min. The AVS process with these parameters leads to the formation a functional and homogenous amine functional layer on the surface of Ti substrates as previously shown [36].

2.2.2. Covalent immobilization of fibronectin on Ti substrates

The extraction of fibronectin was done from cryoprecipitated human plasma as previously described by Poulouin et al. [38] using gelatin-heparin chromatography affinity. This process yielded a fibronectin stock of 500 µg/ml solution in carbonate-bicarbonate buffer. In order to covalently bind fibronectin to the Ti substrates, the stock solution of fibronectin was diluted in 4-morpholine-ethanesulfonic acid (MES, Sigma-Aldrich). AVS-functionalized samples were incubated with the fibronectin-MES solution for 1 h. Subsequently, a solution of N-(3-dimethylaminopropyl)-N′-ethylcarbodiimide hydrochloride (EDC, Sigma-Aldrich)/ N-hydroxysuccinimide (NHS, Aldrich) in MES was added to the samples and incubated for 4 h. The final concentration of the reagents was: fibronectin 200 µg/ml, MES 0.1M pH = 6.0, EDC 0.125 mg/ml and NHS 0.0315 mg/ml.

After incubation, the samples were removed from the solution and gently rinsed with distilled water in order to remove any non-adhered protein from their surface. Subsequently, an intensive cleaning procedure was employed to ensure the complete removal of the excess non-reacted EDC/NHS cross-linkers. The cleaning procedure was established in a previous work with collagen [39] and consisted of incubating the samples in PBS (10 mM, pH = 7.4), MES (0.1 M, pH = 6.0) and Dulbecco's Modified Eagle Medium (DMEM, pH = 7.4) for 5 h, 72 h and 24 h, respectively.

The different conditions assessed in this work are summarized in Table 1.

Table 1. Terminology used for the identification of different samples.

Sample	Details
Ti+AVS+C	AVS-functionalized Ti-6Al-4V incubated with fibronectin and EDC/NHS cross-linkers
Ti+AVS-C	AVS-functionalized Ti-6Al-4V incubated with fibronectin solution without addition of EDC/NHS cross-linkers

 doi:10.20944/preprints202305.1870.v1

Ti+C	Bare Ti-6Al-4V incubated with fibronectin solution and EDC/NHS cross-linkers
Ti-C	Bare Ti-6Al-4V incubated with fibronectin solution without addition of EDC/NHS cross-linkers

2.3. Stability testing

In order to test the stability of covalently bound fibronectin on the surface of Ti substrates, the samples were sonicated in a solution of 10% (w/v) sodium dodecyl sulfate (SDS, Fisher scientific) in PBS for 1 h and incubated in a renewed SDS solution overnight. Finally, the sample were rinsed with distilled water. The rationale behind this procedure was to disrupt any non-covalent bonds in the structure thus, solubilizing and eliminating non-covalently bound fibronectin from the surface of the samples.

2.4. Characterization

2.4.1. Fluorescence microscopy

Fluorescein 5(6)-isothiocyanate (FITC, Fluka) labeling of fibronectin was performed following a method described by Hoffmann et. al. [40]. Briefly, a solution of FITC in anhydrous DMSO was mixed with fibronectin solution (1:100) and the unbound FITC was removed from the solution through gel filtration.

The presence of FITC-labeled fibronectin, whether immobilized or adsorbed, was checked on the substrate surface using fluorescence microscopy (Leica DMI 3000B) at a emission wavelength of 520 nm. Images of the samples were captured both before and after treatment with SDS detergent to assess the stability of the bound fibronectin.

2.4.2. Atomic force microscopy

In order to assess the presence of fibronectin, the surface of the samples was examined by atomic force microscopy (AFM, Cervantes AFM, Nanotec S.L.) before and after the treatment with SDS. The measurements were performed in air using a pyramidal cantilever (Olympus OMCL RC800, semi-angle 39°, nominal resonance frequency 69 KHz) in dynamic mode. The obtained profile data were analyzed by WSxM 5.0 software [41]. Root mean square (RMS) roughness of the samples was calculated from the profile data by WSxM 5.0

2.5. Cell cultures

Murine bone marrow mesenchymal stem cells (BM-MSC) were used as cell model in this study. Isolation and expansion of BM cells were performed on fibronectin-coated wells (Corning Inc., NY) in Iscove's Modified Dulbecco's Medium (IMDM, HyClone) supplemented with 20% of MSC stimulatory supplements (Stem Cell Technologies), 100 µmol/l, 2-mercaptoethanol (Sigma), 100 IU/ml penicillin (Sigma), 0.1 mg/ml streptomycin (GIBCO), 2 mmol/l L-glutamine (GIBCO), 10 ng/ml human PDGF-BB (Peprotech), and 10 ng/ml rm-EGF (Peprotech). Adherent cell clusters were grown for a minimum of 5 passages. After this point, the cells were regularly maintained in DMEM (HyClone) supplemented with 10% fetal bovine serum (FBS, HyClone) and 1% penicillin/streptomycin (Sigma). All the experiments were performed using BM-MSCs in passage 5 through 15.

Prior to cell culture, the samples were sterilized by UV irradiation and put inside the wells of a p24 multiwell. BM-MSCs were seeded on the samples at a concentration of 5×10^4 cells/well and incubated in a humidified atmosphere of 5% CO_2 at 37 ºC for either 4 or 48 h. BM-MSCs cultured on blank wells were used as controls. The experiments were performed twice using duplicate samples.

2.5.1. Cell viability

 doi:10.20944/preprints202305.1870.v1

The viability of cells after 4 and 48 h of seeding was assessed by staining the cells with calcein acetoxymethyl (Calcein AM, Life Technologies, 0.5 μg/μl in DMSO) and propidium iodide (PI, Sigma-Aldrich, 750 μM in PBS). For this purpose, the samples were incubated with a combined solution of 1 μl/ml Calcein/AM and 1 μl/ml PI in DMEM for 30 min. Ultimately, cells were visualized by a fluorescence microscope (Leica DMIRB) at emission wavelengths of 515 and 636 nm for calcein AM and PI, respectively. Three representative images were captured of each sample using a digital camera attached to the microscope (Leica DC100) and the number of viable and PI positive cells were counted in each image using ImageJ software. Results were reported as number of viable cells per mm^2 of the samples surface.

2.5.2. Cell proliferation

Cell proliferation was evaluated at 48 h after seeding on each sample using 2,3-bis-(2-methoxy-4-nitro-5-sulfophenyl)-2H-tetrazolium-5-carboxanilide (XTT, Applichem) according to the manufacturer's instructions. The absorbance of each well was measured spectrophotometrically at 450 nm by an ELX808 microplate reader (BioTeK). The absorbance levels were normalized by the surface area of each sample.

2.5.3. Cell spreading

The morphology of the cells was evaluated at 4 h after seeding. In order to do so, the cells were washed with PBS and fixed in 4% paraformaldehyde, followed by permeabilization using a solution of 0.1% Triton-X100 in PBS. Finally, the cell actin filaments were stained with phalloidin tetramethylrhodamine B isothiocyanate (Phalloidin-TRITC, Sigma) and the nuclei were counterstained with hoechst 33258 (Molecular Probes) by incubating the cells in a combined solution of 2 μg/ml phalloidin and 0.2 mg/ml hoechst in PBS for 60 min at room temperature.

The cells were visualized using a fluorescence microscope (Leica DMIRB) equipped with a digital camera (Leica DC100) at emission wavelengths 570 and 461 nm for phalloidin and hoechst, respectively.

From the obtained images, surface area, perimeter and Feret's diameter of the cells were measured using ImageJ software. 50 individual cells were measured corresponding to each sample.

2.6. Statistical analysis

Statistical analyses were performed using IBM SPSS Statistics 20 software. Statistically significant differences were determined using a one-way ANOVA followed by a Games-Howell post-hoc test. $p < 0.05$ was considered significant. All data are presented as mean value ± standard error.

3. Results

3.1. Evaluation of fibronectin attachment

3.1.1. Fluorescence microscopy

Initially, fluorescence microscopy was employed in order to determine the presence of FITC-labeled fibronectin on the AVS-functionalized and bare Ti samples. The effect of AVS-functionalization (Ti+AVS or Ti) and the presence of cross-linkers (+C or –C) on the immobilization process, was evaluated. The fluorescence microscopy images are shown in Figure 1 after the samples were washed with the SDS solution. Fluorescence is significantly higher in the AVS-functionalized samples compared with the controls (non-functionalized samples). However, no clear difference is apparent from the comparison of the sample incubated with the EDC/NHS crosslinkers (+C) and that not incubated with the crosslinkers (-C). Consequently, it was necessary to use an alternative characterization technique to assess the efficiency of the crosslinking chemistry in contrast with the physical adsorption of the protein on the surface.

Preprints (www.preprints.org) | NOT PEER-REVIEWED | Posted: 26 May 2023 doi:10.20944/preprints202305.1870.v1

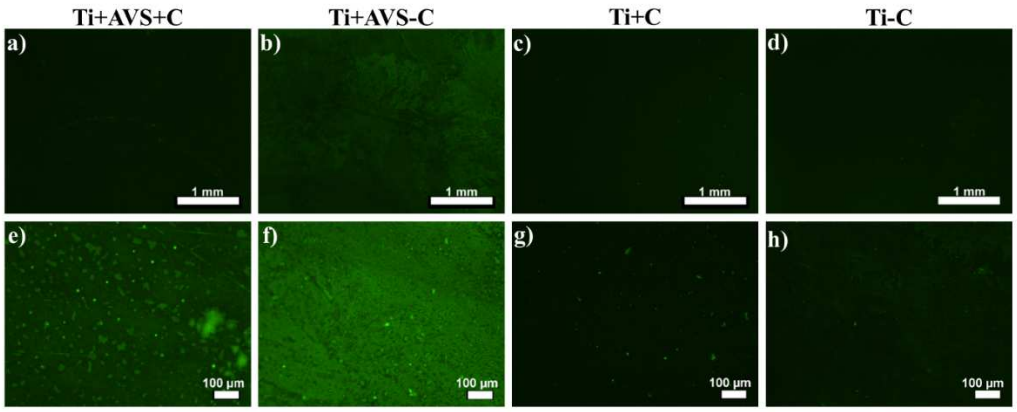

Figure 1. Fluorescence microscopy images of FITC-labeled fibronectin following the classification indicated in Table 1: a,e) Ti+AVS+C, b,f) Ti+AVS-C, c,g) Ti+C and d,h) Ti-C samples in two different magnifications. Samples were incubated with an SDS solution before obtaining the micrographs.

2.1.2. Atomic force microscopy

The surface of all the samples were characterized with AFM to assess the presence and stability of fibronectin on the substrates. AFM topography images of the samples before and after incubation with an SDS solution are shown in Figures 2 and 3, respectively. As previously observed from the fluorescence micrographs, topographic features compatible with the presence of fibronectin on the surface can be clearly seen in the samples Ti+AVS+C and Ti+AVS-C, in contrast with the topography observed in Ti+C and Ti-C samples.

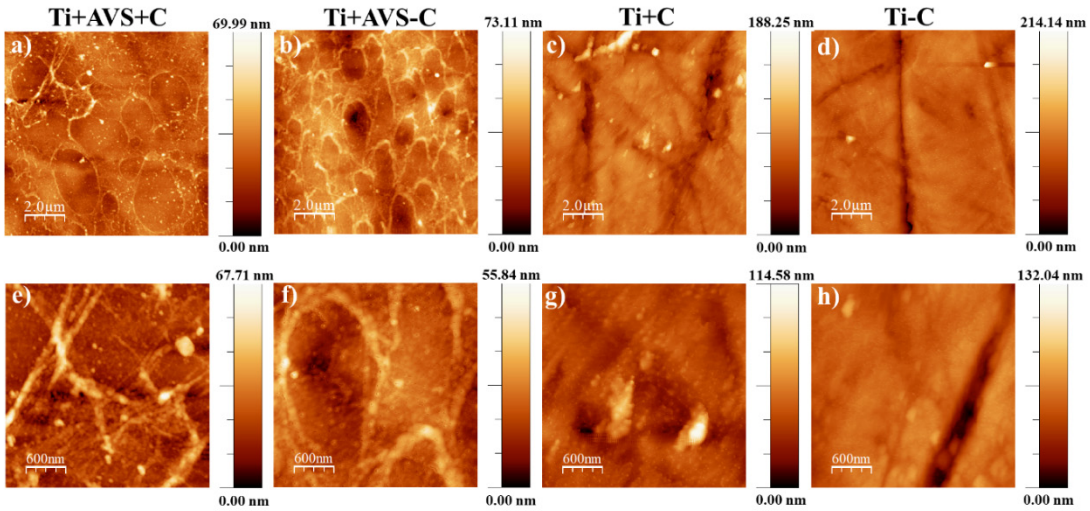

Figure 2. Atomic force microscopy images of a,e) Ti+AVS+C, b,f) Ti+AVS-C, c,g) Ti+C and d,h) Ti-C samples in two different scan sizes. The images follow the classification indicated in Table 1.

Figure 3 shows the AFM topography images of Ti+AVS+C and Ti+AVS-C samples after incubation with an SDS solution. It is evident that, although fibronectin is still present on Ti+AVS+C samples after the treatment, almost all of the fibronectin on Ti+AVS-C samples is removed. Figure 3e presents the RMS roughness values for Ti+AVS+C and Ti+AVS-C samples before and after the treatment with SDS. It can be seen that while the roughness for Ti+AVS+C does not change significantly after the treatment with SDS, there is a marked decrease in the roughness of Ti+AVS-C samples indicating removal of fibronectin from these samples. Altogether, these results are a clear indication of the higher stability of the covalently immobilized fibronectin when compared with the physically adsorbed protein.

Preprints (www.preprints.org) | NOT PEER-REVIEWED | Posted: 26 May 2023 doi:10.20944/preprints202305.1870.v1

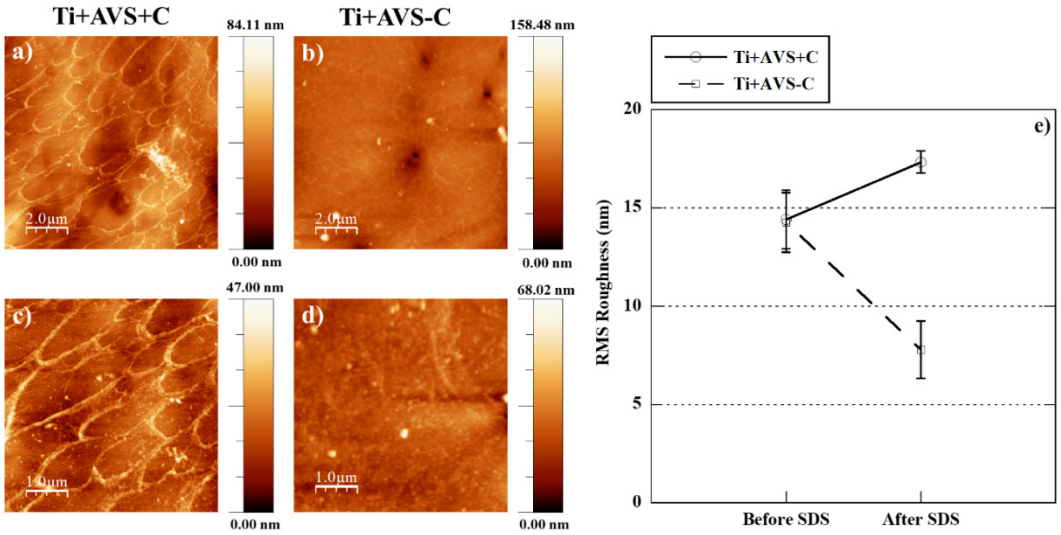

Figure 3. Atomic force microscopy images of a,c) Ti+AVS+C, b,d) Ti+AVS-C samples after treatment with SDS in two different scan sizes and e) RMS roughness of Ti+AVS+C and Ti+AVS-C samples before and after treatment with SDS. The images follow the classification indicated in Table 1.

3.2. Biological assessment

3.2.1. Cell adhesion and proliferation

The biological response of fibronectin-immobilized (Ti+AVS+C) samples was assessed by performing in-vitro cultures of murine bone marrow mesenchymal stem cells (BM-MSCs). Figure 4 shows the morphology of the BM-MSCs adhered to bare Ti, fibronectin-decorated Ti and polystyrene control samples at 4 and 48 h after seeding. At 4 h after seeding, the cells adhered to fibronectin-immobilized samples showed a higher expansion of the cytoskeleton compared to those on bare Ti. At 48 h of seeding, the cells on fibronectin-decorated Ti showed a better cell arrangement, more developed processes, and extended filopodia compared to those observed on bare Ti.

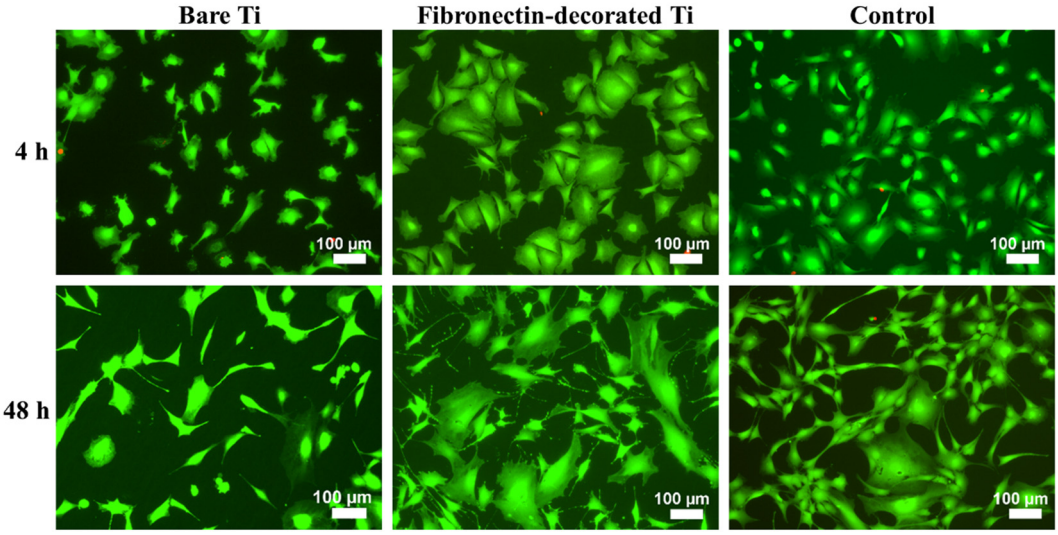

Figure 4. Fluorescence microscopy images of calcein/PI stained BM-MSCs adhered to bare Ti, fibronectin-decorated Ti and polystyrene control samples at 4 h and 48 h after seeding. Viable cells are stained green, whilst the dead cells appear as red events.

Preprints (www.preprints.org) | NOT PEER-REVIEWED | Posted: 26 May 2023 doi:10.20944/preprints202305.1870.v1

The number of calcein positive cells counted on each sample is shown in Figure 5a. It can be seen that at either 4 or 48 h after seeding a significantly higher number of cells are adhered on the fibronectin-decorated Ti samples compared to bare Ti (p-value = 0.009 and 0.002 for 4 and 48 h, respectively).

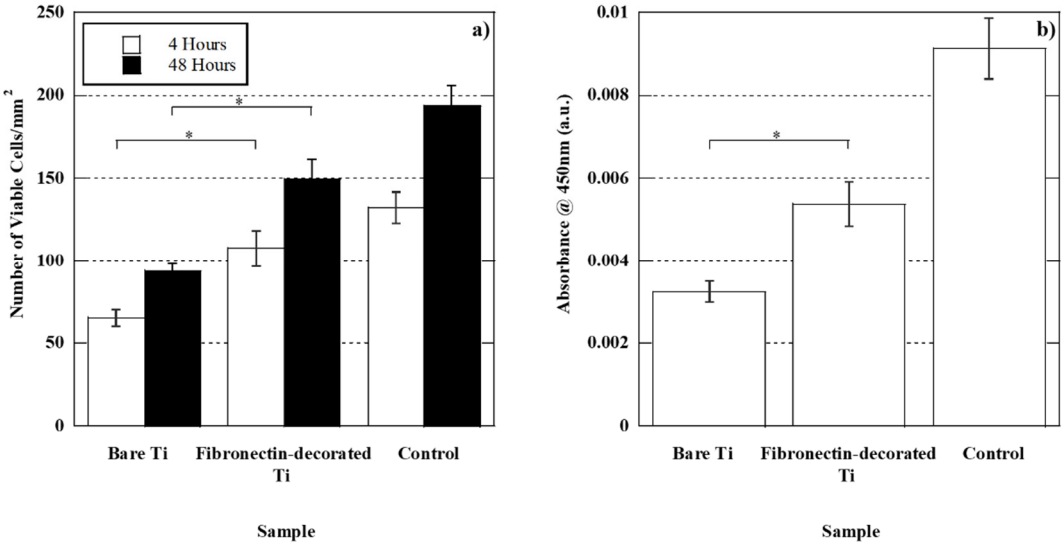

Figure 5. Number of BM-MSCs on bare Ti, fibronectin-decorated Ti and polystyrene control samples obtained by a) cell counting from micrographs after 4 and 48 h of seeding, b) XTT measurement 48 h after seeding. * depicts statistically significant difference.

The results of independent XTT assays after 48 h of seeding (Figure 5b) confirmed that the fibronectin-decorated Ti samples possessed significantly more metabolically active cells compared to bare Ti (p-value = 0.013).

3.2.2. Cell morphology and spreading

The fluorescence images of phalloidin/hoeschst stained BM-MSC cells adhered on bare Ti, fibronectin-decorated Ti and polystyrene control samples at 4 h after seeding can be seen in Figure 6. The cells adhered on fibronectin-decorated Ti samples exhibited a more mature and developed actin cytoskeleton compared to those adhered on bare Ti samples.

Quantitative measurements of cell surface area shown in Figure 7a revealed that the cells adhered on bare Ti samples possess the smallest surface area. The cells adhered on the fibronectin-decorated Ti samples possessed a significantly larger surface area, almost three times larger than that of the cells on bare Ti (p-value = 0.0001), a value comparable to that found in the polystyrene control samples. A similar trend was observed with respect to the cell perimeter and Feret's diameter between cells cultured on the fibronectin-decorated samples and those on control bare Ti.

Preprints (www.preprints.org) | NOT PEER-REVIEWED | Posted: 26 May 2023 doi:10.20944/preprints202305.1870.v1

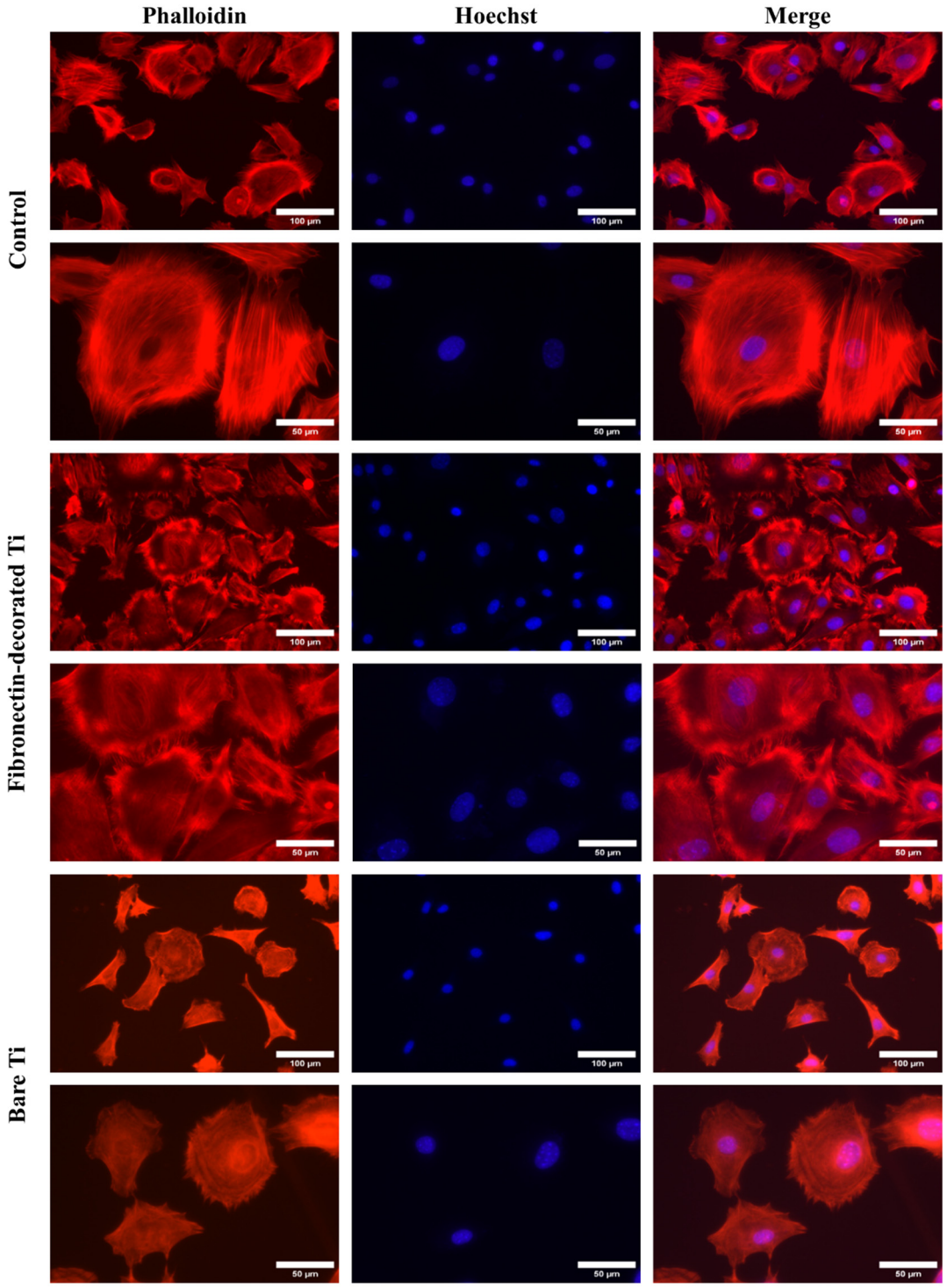

Figure 6. Fluorescence microscopy images of phalloidin/hoechst stained BM-MSCs adhered to bare Ti, fibronectin-decorated Ti and polystyrene control samples 4 h after seeding at two different magnifications.

Preprints (www.preprints.org) | NOT PEER-REVIEWED | Posted: 26 May 2023 doi:10.20944/preprints202305.1870.v1

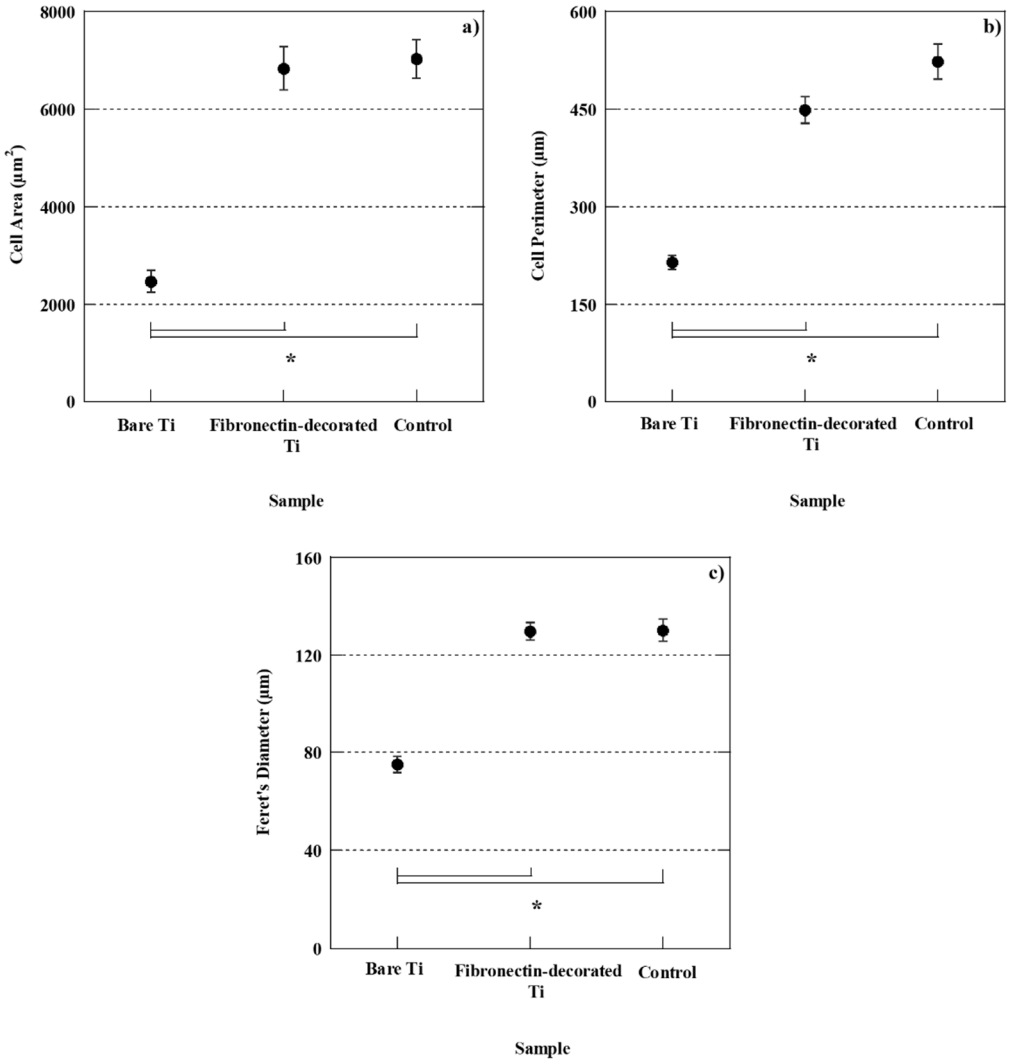

Figure 7. Cell surface area a), cell perimeter b), and cell Feret's diameter c) of BM-MSCs adhered to bare Ti, fibronectin-decorated Ti and polystyrene control samples at 4 h after seeding. * indicates statistically significant difference.

4. Discussion

In the present study, a robust biofunctionalization procedure was used to covalently bind fibronectin to the surface of a solid biomaterial. A thin functionalized layer was deposited on the surface of the Ti substrate using AVS [37,42]. The amines present on the surface of the thin layer were used to covalently bind fibronectin with the EDC/NHS crosslinking chemistry. A scheme of the covalent linking of fibronectin on the surfaces is shown in Figure 8.

Preprints (www.preprints.org) | NOT PEER-REVIEWED | Posted: 26 May 2023 doi:10.20944/preprints202305.1870.v1

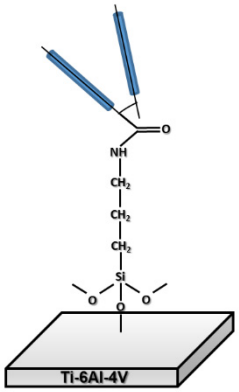

Figure 8. Scheme of the covalent binding of fibronectin to the functionalized titanium substrate.

The presence of fibronectin on the surface of the functionalized samples was initially established with fluorescence microscopy and, subsequently, confirmed through AFM micrographs. In order to verify the covalent immobilization of fibronectin on Ti+AVS+C samples, a process of elution with SDS was applied, since the detergent SDS is commonly used to eliminate weak interactions between proteins. The AFM topography images recorded after the treatment with SDS clearly confirmed that fibronectin was only present on Ti+AVS+C samples, whereas it was removed from the surface of Ti+AVS-C samples (i.e. not incubated with the EDC/NHS crsosslinkers). The presence of significant amount of fibronectin on the Ti+AVS-C before being immersed in an SDS solution can be explained by considering the possible electrostatic interaction between the functionalized substrate and fibronectin. The isoelectric point of fibronectin is reported to be pI = 5.2 [43]. In this case, at the pH = 6.0 in which the experiments were performed, fibronectin will be negatively charged, while the surface of AVS-functionalized samples is positively charged due to the presence of primary/secondary amines. The attraction forces generated between the surface amines and fibronectin may lead to the adsorption of relatively high amounts of fibronectin on the surface of the samples. In contrast, non-functionalized samples (Ti+C and Ti-C) present a TiO_2 layer on the surface [44], and, since this oxide layer is negatively charged at pH = 6.0 [45,46], the repulsion forces between the surface of the Ti+C and Ti-C samples and fibronectin must largely prevent the physical adsorption of fibronectin to the surface of the material.

The response of BM-MSCs to the covalently bound fibronectin on Ti samples was also addressed. It was demonstrated that a significantly higher number of cells was measured on the fibronectin-decorated Ti than on bare Ti samples at 4 h after seeding. This trend was also found in the analysis performed at 48 h after seeding.

It has been reported that the mechanisms involved in the interaction of fibronectin with cells are based on the recognition by integrins [47] of cell adhesion motifs, such as RGD [48–50], PHSRN (Proline – Histidine – Serine – Arginine – Asparagine) [19,51], LDV (Leucine – Aspartic acid – Valine) [21] and REDV (Arginine – Glutamate – Aspartic acid – Valine) [20], that appear in the sequence of fibronectin. Consequently, it may be hypothesized that some or all of these motifs may contribute to the enhanced proliferation of BM-MSC on the fibronectin-decorated substrates.

Moreover, an enhanced adhesion of the cells on the substrate may tailor the interaction between these and the material. In this regard, it is acknowledged that proliferation of substrate-dependent cells is highly affected by the extension of the cells on the material. For instance, it was found that the lack of sufficient spreading on a substrate can even cause apoptosis in the cells [52]. Alternatively, it is also hypothesized that initial cell spreading magnitude may have a positive influence on the subsequent cell proliferation [53–55], as a consequence of two mechanisms that might be involved in this process. The first mechanism establishes that cells with a higher surface area are able to uptake higher amount of protein from the biological fluids. This higher protein uptake induces the transition of the cells from G0 to G1 and from G1 to S phase of the cell cycle and favors cell proliferation [56–

59]. The second mechanism is based on mechanical cues, as sensed by the actin cytoskeleton. As the cells expand on the substrate, the stress in the actin fibers increases. The increase in stress in the actin fibers would prompt the stimulation of cell proliferation through DNA synthesis and nuclear expansion [60–63]. Therefore, an enhanced initial cell spreading by virtue of covalent binding of fibronectin to AVS-functionalized implant could improve subsequent cell proliferation and, possibly, the integration of the material in the recipient organism due to the possible enlarged tissue-implant contact area. Elongated cells with high Feret's diameter as observed on the fibronectin-decorated Ti samples, suggest a highly expanded cytoskeleton with stretched actin fibers which is favorable for cell proliferation.

5. Conclusions

In this study, fibronectin was covalently bound to a functionalized Ti substrate through the EDC/NHS cross-linking chemistry. The presence of the fibronectin on the surface was characterized by fluorescence microscopy and by AFM. It is demonstrated that higher amounts of fibronectin were present on functionalized samples compared with bare Ti (control) samples. The robustness of the procedure was confirmed by the resistance of the immobilized fibronectin to incubation in SDS. In-vitro cell cultures revealed that the covalent binding of fibronectin on Ti surface improves initial cell adhesion and spreading of BM-MCSs compared with bare Ti samples, reaching values comparable to the polystyrene controls. In summary, the results discussed in this work represent a robust approach for the covalent immobilization of fibronectin in order to enhance the biological response of a wide range of biomaterials. The versatility of this procedure implies that this methodology could pave the way for the development of novel implants with improved biological properties in the future.

Author Contributions: PR performed the experimental work with the help of AA-L and RT, and prepared the first version of the manuscript. RD and LC performed the AFM analysis. ME, GVG and DG-N contributed to the analysis of the data. The work was coordinated by JP-R. All authors have read and agreed to the published version of the manuscript.

Funding: This study was partially funded by the Ministerio de Ciencia e Innovación (PID2020-116403RB-I00) and by the Comunidad de Madrid (Spain) (MINA-CM P2022-BMD-7236, PIN1-00011.2/2022_INVESTIGO_CM, Tec4Bio-CM/P2018/NMT-4443 and PEJ-2021-AI/IND-21188). This work was funded by the European Union's EIC-Pathfinder Programme, under the project THOR (Grant Agreement number 101099719).

Data Availability Statement: Data are available upon request to the corresponding author.

Conflicts of Interest: The authors declare no conflict of interest."

References

1. Brunette, D.M.; Tengvall, P.; Textor, M.; Thomsen, P. Titanium in medicine: material science, surface science, engineering, biological responses and medical applications; Springer Science & Business Media, 2012.
2. Liu, X.; Chu, P.K.; Ding, C. Surface modification of titanium, titanium alloys, and related materials for biomedical applications. *Mater. Sci. Eng. R Rep* **2004**, 47, 49-121.
3. Chen, Q.; Thouas, G.A. Metallic implant biomaterials. *Mater. Sci. Eng. R Rep* **2015**, 87, 1-57.
4. Geetha, M.; Singh, A.K.; Asokamani, R.; Gogia, A.K. Ti based biomaterials, the ultimate choice for orthopaedic implants – A review. *Prog. Mater. Sci.* **2009**, 54, 397-425.
5. Ratner, B.D.; Hoffman, A.S.; Schoen, F.J.; Lemons, J.E. *Biomaterials Science: An Introduction to Materials in Medicine*; Elsevier Science, 2004.
6. Coleman, D.L.; King, R.N.; Andrade, J.D. The foreign body reaction: a chronic inflammatory response. *J. Biomed. Mater. Res.* **1974**, 8, 199-211.
7. Santavirta, S.; Gristina, A.; Konttinen, Y.T. Cemented versus cementless hip arthroplasty. A review of prosthetic biocompatibility. *Acta Orthop. Scand.* **1992**, 63, 225-232.
8. Agarwal, R.; Garcia, A.J. Biomaterial strategies for engineering implants for enhanced osseointegration and bone repair. *Adv. Drug Deliv. Rev.* **2015**, 94, 53-62.
9. Stich, T.; Alagboso, F.; Křenek, T.; Kovářík, T.; Alt, V.; Docheva, D. Implant-bone-interface: Reviewing the impact of titanium surface modifications on osteogenic processes in vitro and in vivo. *Bioeng. Transl. Med.* **2022**, 7, e10239.

10. Wroblewski, B.M. Current trends in revision of total hip arthroplasty. *Int. Orthop.* **1984**, 8, 89-93.
11. Hanawa, T. Titanium–Tissue Interface Reaction and Its Control With Surface Treatment. *Front. Bioeng. Biotechnol.* **2019**, 7.
12. Marín-Pareja, N.; Salvagni, E.; Guillem-Marti, J.; Aparicio, C.; Ginebra, M. Collagen-functionalised titanium surfaces for biological sealing of dental implants: Effect of immobilisation process on fibroblasts response. *Colloids Surf. B: Biointerfaces* **2014**, 122, 601-610.
13. Kurth, D.G.; Bein, T. Thin Films of (3-Aminopropyl)triethoxysilane on Aluminum Oxide and Gold Substrates. *Langmuir* **1995**, 11, 3061-3067.
14. Trino, L.D.; Bronze-Uhle, E.S.; George, A.; Mathew, M.T.; Lisboa-Filho, P.N. Surface Physicochemical and Structural Analysis of Functionalized Titanium Dioxide Films. *Colloids Surf. Physicochem. Eng. Aspects* **2018**, 546, 168-178.
15. Celesti, C.; Gervasi, T.; Cicero, N.; Giofrè, S.V.; Espro, C.; Piperopoulos, E.; Gabriele, B.; Mancuso, R.; Lo Vecchio, G.; Iannazzo, D. Titanium Surface Modification for Implantable Medical Devices with Anti-Bacterial Adhesion Properties. *Materials* **2022**, 15.
16. White, L.D.; Tripp, C.P. Reaction of (3-Aminopropyl)dimethylethoxysilane with Amine Catalysts on Silica Surfaces. *J. Colloid Interface Sci.* **2000**, 232, 400-407.
17. Arkles, B.; Steinmetz, J.R.; Zazyczny, J.; Mehta, P. Factors contributing to the stability of alkoxysilanes in aqueous solution. *J. Adhes. Sci. Technol.* **1992**, 6, 193-206.
18. Vogel, V.; Thomas, W.E.; Craig, D.W.; Krammer, A.; Baneyx, G. Structural insights into the mechanical regulation of molecular recognition sites. *Trends Biotechnol.* **2001**, 19, 416-423.
19. Aota, S.; Nomizu, M.; Yamada, K.M. The short amino acid sequence Pro-His-Ser-Arg-Asn in human fibronectin enhances cell-adhesive function. *J. Biol. Chem.* **1994**, 269, 24756-24761.
20. Humphries, M.J.; Akiyama, S.K.; Komoriya, A.; Olden, K.; Yamada, K.M. Identification of an alternatively spliced site in human plasma fibronectin that mediates cell type-specific adhesion. *J. Cell Biol.* **1986**, 103, 2637-2647.
21. Komoriya, A.; Green, L.J.; Mervic, M.; Yamada, S.S.; Yamada, K.M.; Humphries, M.J. The minimal essential sequence for a major cell type-specific adhesion site (CS1) within the alternatively spliced type III connecting segment domain of fibronectin is leucine-aspartic acid-valine. *J. Biol. Chem.* **1991**, 266, 15075-15079.
22. Benoit, D.S.W.; Anseth, K.S. The effect on osteoblast function of colocalized RGD and PHSRN epitopes on PEG surfaces. *Biomaterials* **2005**, 26, 5209-5220.
23. Hsiao, C.; Cheng, H.; Huang, C.; Li, H.; Ou, M.; Huang, J.; Khoo, K.; Yu, H.W.; Chen, Y.; Wang, Y.; Chiou, A.; Kuo, J. Fibronectin in cell adhesion and migration via N-glycosylation. *Oncotarget* **2017**, 8, 70653-70668.
24. Ruoslahti, E. Fibronectin in cell adhesion and invasion. *Cancer Metastasis Rev.* **1984**, 3, 43-51.
25. Seitz, T.L.; Noonan, K.D.; Hench, L.L.; Noonan, N.E. Effect of fibronectin on the adhesion of an established cell line to a surface reactive biomaterial. *J. Biomed. Mater. Res.* **1982**, 16, 195-207.
26. Dessau, W.; Sasse, J.; Timpl, R.; Jilek, F.; von der Mark, K. Synthesis and extracellular deposition of fibronectin in chondrocyte cultures. Response to the removal of extracellular cartilage matrix. *J. Cell Biol.* **1978**, 79, 342-355.
27. Rapuano, B.E.; MacDonald, D.E. Surface oxide net charge of a titanium alloy: Modulation of fibronectin-activated attachment and spreading of osteogenic cells. *Colloids Surf. B: Biointerfaces* **2011**, 82, 95-103.
28. Ku, Y.; Chung, C.; Jang, J. The effect of the surface modification of titanium using a recombinant fragment of fibronectin and vitronectin on cell behavior. *Biomaterials* **2005**, 26, 5153-5157.
29. Säuberlich, S.; Klee, D.; Richter, E.; Höcker, H.; Spiekermann, H. Cell culture tests for assessing the tolerance of soft tissue to variously modified titanium surfaces. *Clin. Oral Implants Res.* **1999**, 10, 379-393.
30. Cannas, M.; Denicolai, F.; Webb, L.X.; Gristina, A.G. Bioimplant surfaces: binding of fibronectin and fibroblast adhesion. *J. Orthop. Res.* **1988**, 6, 58-62.
31. Sugita, Y.; Saruta, J.; Taniyama, T.; Kitajima, H.; Hirota, M.; Ikeda, T.; Ogawa, T. UV-Pre-Treated and Protein-Adsorbed Titanium Implants Exhibit Enhanced Osteoconductivity. *Int. J. Mol. Sci.* **2020**, 21.
32. Ghadhab, S.; Bilem, I.; Guay-Bégin, A.; Chevallier, P.; Auger, F.A.; Ruel, J.; Pauthe, E.; Laroche, G. Fibronectin grafting to enhance skin sealing around transcutaneous titanium implant. *J. Biomed. Mater. Res.* **2021**, 109, 2187-2198.
33. Pugdee, K.; Shibata, Y.; Yamamichi, N.; Tsutsumi, H.; Yoshinari, M.; Abiko, Y.; Hayakawa, T. Gene expression of MC3T3-E1 cells on fibronectin-immobilized titanium using tresyl chloride activation technique. *Dent. Mater. J.* **2007**, 26, 647-655.
34. Hayakawa, T.; Yoshida, E.; Yoshimura, Y.; Uo, M.; Yoshinari, M. MC3T3-E1 Cells on Titanium Surfaces with Nanometer Smoothness and Fibronectin Immobilization. *Int. J. Biomater.* **2012**, 2012, 6.
35. Pham, M.T.; Reuther, H.; Maitz, M.F. Native extracellular matrix coating on Ti surfaces. *J. Biomed. Mater. Res. A* **2003**, 66A, 310-316.
36. Martín-Palma, R.J.; Manso, M.; Pérez-Rigueiro, J.; García-Ruiz, J.P.; Martínez-Duart, J.M. Surface biofunctionalization of materials by amine groups. *J. Mater. Res.* **2004**, 19, 2415-2420.

37. Rezvanian, P.; Arroyo-Hernández, M.; Ramos, M.; Daza, R.; Elices, M.; Guinea, G.V.; Pérez-Rigueiro, J. Development of a versatile procedure for the biofunctionalization of Ti-6Al-4V implants. *Appl. Surf. Sci.* **2016**, 387, 652-660.
38. Poulouin, L.; Gallet, O.; Rouahi, M.; Imhoff, J. Plasma Fibronectin: Three Steps to Purification and Stability. *Protein Expr. Purif.* **1999**, 17, 146-152.
39. Rezvanian, P.; Daza, R.; López, P.A.; Ramos, M.; González-Nieto, D.; Elices, M.; Guinea, G.V.; Pérez-Rigueiro, J. Enhanced Biological Response of AVS-Functionalized Ti-6Al-4V Alloy through Covalent Immobilization of Collagen. *Sci. Rep.* **2018**, 8, 3337.
40. Hoffmann, C.; Leroy-Dudal, J.; Patel, S.; Gallet, O.; Pauthe, E. Fluorescein isothiocyanate-labeled human plasma fibronectin in extracellular matrix remodeling. *Anal. Biochem.* **2008**, 372, 62-71.
41. Horcas, I.; Fernández, R.; Gómez-Rodríguez, J.M.; Colchero, J.; Gómez-Herrero, J.; Baro, A.M. WSXM: A software for scanning probe microscopy and a tool for nanotechnology. *Rev. Sci. Instrum.* **2007**, 78, 013705.
42. Arroyo-Hernandez, M.; Martin-Palma, R.J.; Perez-Rigueiro, J.; Garcia-Ruiz, J.P.; Garcia-Fierro, J.L.; Martinez-Duart, J.M. Biofunctionalization of surfaces of nanostructured porous silicon. *Mater. Sci. Eng. C* **2003**, 23, 697-701.
43. Tooney, N.M.; Mosesson, M.W.; Amrani, D.L.; Hainfeld, J.F.; Wall, J.S. Solution and surface effects on plasma fibronectin structure. *J. Cell Biol.* **1983**, 97, 1686-1692.
44. Rinner, M.; Gerlach, J.; Ensinger, W. Formation of titanium oxide films on titanium and Ti6Al4V by O2-plasma immersion ion implantation. *Surf. Coat. Technol.* **2000**, 132, 111-116.
45. Rodríguez-Sánchez, J.; Gallardo-Moreno, A.M.; Bruque, J.M.; González-Martín, M.L. Adsorption of human fibrinogen and albumin onto hydrophobic and hydrophilic Ti6Al4V powder. *Appl. Surf. Sci.* **2016**, 376, 269-275.
46. MacDonald, D.E.; Rapuano, B.E.; Schniepp, H.C. Surface Oxide Net Charge of a Titanium Alloy; Comparison Between Effects of Treatment With Heat or Radiofrequency Plasma Glow Discharge. *Colloids Surf. B: Biointerfaces* **2010**, 82, 173-181.
47. Parisi, L.; Toffoli, A.; Ghezzi, B.; Mozzoni, B.; Lumetti, S.; Macaluso, G.M. A glance on the role of fibronectin in controlling cell response at biomaterial interface. *Jpn. Dent. Sci. Rev.* **2020**, 56, 50-55.
48. Brighton, C.T.; Albelda, S.M. Identification of integrin cell-substratum adhesion receptors on cultured rat bone cells. *J. Orthop. Res.* **1992**, 10, 766-773.
49. Miyamoto, S.; Katz, B.Z.; Lafrenie, R.M.; Yamada, K.M. Fibronectin and integrins in cell adhesion, signaling, and morphogenesis. *Ann. N. Y. Acad. Sci.* **1998**, 857, 119-129.
50. Hersel, U.; Dahmen, C.; Kessler, H. RGD modified polymers: biomaterials for stimulated cell adhesion and beyond. *Biomaterials* **2003**, 24, 4385-4415.
51. Oliver-Cervelló, L.; Martin-Gómez, H.; Mas-Moruno, C. New trends in the development of multifunctional peptides to functionalize biomaterials. *J. Pep. Sci.* **2022**, 28, e3335.
52. Straface, E.; Natalini, B.; Monti, D.; Franceschi, C.; Schettini, G.; Bisaglia, M.; Fumelli, C.; Pincelli, C.; Pellicciari, R.; Malorni, W. C3-fullero-tris-methanodicarboxylic acid protects epithelial cells from radiation-induced anoikia by influencing cell adhesion ability. *FEBS Lett.* **1999**, 454, 335-340.
53. Thomas, C.H.; Lhoest, J.B.; Castner, D.G.; McFarland, C.D.; Healy, K.E. Surfaces designed to control the projected area and shape of individual cells. *J. Biomech. Eng.* **1999**, 121, 40-48.
54. Chen, C.S.; Mrksich, M.; Huang, S.; Whitesides, G.M.; Ingber, D.E. Geometric control of cell life and death. *Science* **1997**, 276, 1425-1428.
55. Huang, S.; Chen, C.S.; Ingber, D.E. Control of cyclin D1, p27(Kip1), and cell cycle progression in human capillary endothelial cells by cell shape and cytoskeletal tension. *Mol. Biol. Cell* **1998**, 9, 3179-3193.
56. Avraham, H.K.; Lee, T.H.; Koh, Y.; Kim, T.A.; Jiang, S.; Sussman, M.; Samarel, A.M.; Avraham, S. Vascular endothelial growth factor regulates focal adhesion assembly in human brain microvascular endothelial cells through activation of the focal adhesion kinase and related adhesion focal tyrosine kinase. *J. Biol. Chem.* **2003**, 278, 36661-36668.
57. Dwivedi, A.; Sala-Newby, G.B.; George, S.J. Regulation of cell-matrix contacts and beta-catenin signaling in VSMC by integrin-linked kinase: implications for intimal thickening. *Basic Res. Cardiol.* **2008**, 103, 244-256.
58. Zamir, E.; Geiger, B. Molecular complexity and dynamics of cell-matrix adhesions. *J. Cell. Sci.* **2001**, 114, 3583-3590.
59. Khetan, J.; Shahinuzzaman, M.; Barua, S.; Barua, D. Quantitative Analysis of the Correlation between Cell Size and Cellular Uptake of Particles. *Biophys. J.* **2019**, 116, 347-359.
60. Assoian, R.K.; Klein, E.A. Growth control by intracellular tension and extracellular stiffness. *Trends. Cell. Biol.* **2008**, 18, 347-352.
61. Bacakova, L.; Filova, E.; Parizek, M.; Ruml, T.; Svorcik, V. Modulation of cell adhesion, proliferation and differentiation on materials designed for body implants. *Biotechnol. Adv.* **2011**, 29, 739-767.
62. Ingber, D.E.; Prusty, D.; Sun, Z.; Betensky, H.; Wang, N. Cell shape, cytoskeletal mechanics, and cell cycle control in angiogenesis. *J. Biomech.* **1995**, 28, 1471-1484.

 doi:10.20944/preprints202305.1870.v1

63. Hoffman, L.M.; Smith, M.A.; Jensen, C.C.; Yoshigi, M.; Blankman, E.; Ullman, K.S.; Beckerle, M.C. Mechanical stress triggers nuclear remodeling and the formation of transmembrane actin nuclear lines with associated nuclear pore complexes. *Mol. Biol. Cell* **2020**, 31, 1774-1787.